

# Closed Form Integration of Gravity-Capillary Rings

## Supplementary Material for SIGGRAPH 2019

CHRISTIAN HAFNER, IST Austria

CHRIS WOJTAN, IST Austria

### 1 INTRODUCTION

This document describes in detail how to simulate circular ripples using approximate fundamental solutions to the linear deep water wave equations. Our work builds heavily upon the work of Le Méhauté [1988], which was the first to analyze the behavior of water rings like raindrops. The fundamental solution is too complicated to be derived analytically, so we apply multiple approximations, namely Taylor series expansions and the method of stationary phase for approximating oscillatory integrals, in order to get an analytic expression that well-approximates the behavior of concentric circular water ripples. The resulting analytic function can be used to simulate and render hundreds of detailed raindrops at faster than real-time rates. The resulting ripple animations exhibit arbitrarily high-resolution visual details and are free from visual artifacts, even when zooming in close to the scene.

Section 2 formalizes the problem and presents the exact mathematical solution, which does not lend itself to direct computation. Section 3 presents two analytical approximations: one as a simple sum of two-waves, and one for trailing edge of the wave. Finally, Section 4 discusses the implementation of a real-time graphics demo to showcase the closed-form raindrop ripple approximation. All formulae that are needed for implementation are summarized in the appendix for reference.

### 2 BACKGROUND

Le Méhauté describes the gravity-capillary rings caused by a small impact on a liquid surface such as the one generated by a raindrop [Le Méhauté 1988]. Here, we summarize the problem's formalization as a linear dissipative axisymmetric wave equation with surface tension and present the exact solution.

The equations of the system are written in terms of the velocity potential  $\phi(r, z, t)$ , and the free surface height  $u(r, t)$ . The independent variables are the radius  $r$  (distance from the impact), the vertical coordinate  $z$ , and time  $t$ . The governing equations are

$$\phi_t = -u + \tau \left( u_{rr} + \frac{1}{r} u_r \right), \quad u_t = \phi_z.$$

The factor multiplying  $\tau$  accounts for surface tension and arises as the Laplacian of  $u$  in cylindrical coordinates after eliminating derivatives with respect to the angular coordinate due to axisymmetry.

The general solution for the free surface is

$$u(r, t) = \int_0^\infty J_0(k, r) [A(k) \cos(\omega t) - B(k) \sin(\omega t)] \omega k dk,$$

where  $J_0$  is the Bessel function of the first kind and order zero. The dispersion relationship linking the angular frequency  $\omega$  to the

wavenumber  $k$  is

$$\omega^2 = k \left( 1 + \tau k^2 \right).$$

Two initial conditions are needed to determine  $\eta$ . The first is chosen as  $u(\cdot, 0) \equiv 0$ , corresponding to an initially planar water surface. This leads to  $A \equiv 0$ . The second initial condition models the initial impulse as a parabolic pressure distribution limited to the size of the disturbance. This distribution is chosen for mathematical convenience, and because the authors found its exact shape to be of little consequence. Eventually, this choice leads to

$$B(k) \sim \frac{J_2(k)}{k^2}.$$

The final expression for the free surface is then

$$\theta(r, t) = \int_0^\infty \frac{\omega}{k} J_2(k) J_0(kr) \sin(\omega t) dk, \quad (1)$$

where  $\theta \sim u$ .

To account for dissipation effects, the integrand is further multiplied by a damping coefficient

$$D(k, t) = \exp[-\gamma(k)t],$$

where  $\gamma$  combines the effects of a contaminated surface boundary layer and internal strain. The former tends to dominate the dissipation process, and scales as  $\gamma \sim k^{7/4}$ . This term is responsible for the characteristic shape of raindrop ripples as it determines the relative amplitudes of low-frequency gravity waves and high-frequency capillary waves. Initially, both types of waves are visible, but a few seconds after impact, high wavenumbers  $k$  are strongly damped and gravity waves dominate the picture.

### 3 APPROXIMATE SOLUTION

Eq. 1 is an oscillating integral, and the frequency of the integrand is increasing in  $k$ . This makes the problem ill-suited for numerical integration by quadrature, as many samples are necessary to obtain valid approximations. To obtain a solution, the authors make two approximations.

The first is to substitute  $J_2(k)$  by its second-order Taylor expansion at  $k = 0$ , which gives  $\frac{1}{8}k^2$ . This is justified because it will be small values of  $k$  that matter: large wave numbers are too heavily damped to make a contribution. The argument is consistent with observations, as replacing  $J_2(k)$  with the approximation yields a visually indistinguishable result.

The second is a stationary phase approximation of the integral. This method is based on the observation that contributions of an oscillating integral largely cancel out except for those around local extrema of the phase function. Thus, it is justifiable to expand the phase as a sum of Taylor series about the extrema and to neglect higher-order terms.

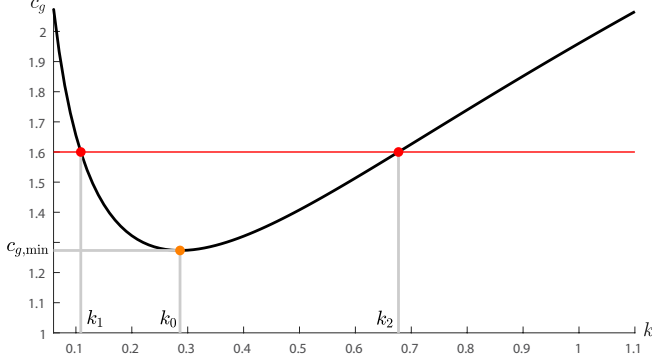


Fig. 1. Group speed  $c_g$  as a function of wavenumber  $k$  in black. Example group speed and pair of critical wavenumbers  $k_1, k_2$  in red. Minimum group speed  $c_{g,\min}$  and corresponding wavenumber  $k_0$  in orange.

The oscillatory factors in Eq. 1 are  $J_0(kr) \sin(\omega t)$ . The Bessel function is approximated by an asymptotic form

$$J_0(kr) \approx \sqrt{\frac{2}{\pi kr}} \sin\left(kr + \frac{\pi}{4}\right),$$

which is accurate away from the origin. The product can then be written as

$$J_0(kr) \sin(\omega t) \approx \sqrt{\frac{1}{2\pi kr}} \left( \cos\left(\omega t - kr - \frac{\pi}{4}\right) - \cos\left(\omega t + kr + \frac{\pi}{4}\right) \right).$$

The phase of the second term,  $\omega t + kr + \frac{\pi}{4}$ , does not attain an extremum within the integration limits, so it can be dropped in the stationary phase approximation. This leaves the phase  $\phi(k) = \omega t - kr - \frac{\pi}{4}$ , which attains an extremum where

$$0 = \frac{d\phi}{dk} = \frac{d\omega}{dk}t - r, \quad \text{or where} \quad \frac{d\omega}{dk} =: c_g = \frac{r}{t}.$$

The group speed  $c_g$  has a global minimum  $c_{g,\min} = c_g(k_0)$  and tends to infinity monotonically for  $k \rightarrow 0$  and for  $k \rightarrow \infty$ . Thus, for  $c_g > c_{g,\min}$ , there are exactly two wavenumbers that render the phase stationary. For  $c_g < c_{g,\min}$ , the phase is nowhere stationary, and there is no significant contribution to the integral. The point  $c_{g,\min} = \frac{r}{t}$  marks the trailing edge of the wave, see Fig. 1.

For the case  $\frac{r}{t} > c_{g,\min} + \varepsilon$ , which is away from the trailing edge, the two wavenumbers that render the phase stationary are well separated. This inequality holds for most of the wave's spatial extent, and treating only this case suffices for computer animation purposes. For completion's sake, we also describe an approximation for  $\frac{r}{t} \approx c_{g,\min}$  further below. Both approximations are shown in Fig. 2, overlaid on the ground truth obtained via numerical quadrature with a high sample count.

### 3.1 Two-wave approximation

Away from the trailing edge, there are two wavenumbers  $k_1, k_2$  that render the phase function  $\phi$  stationary or, equivalently, where  $c_g = \frac{r}{t}$ . The free surface in Eq. 1, after introducing damping and the

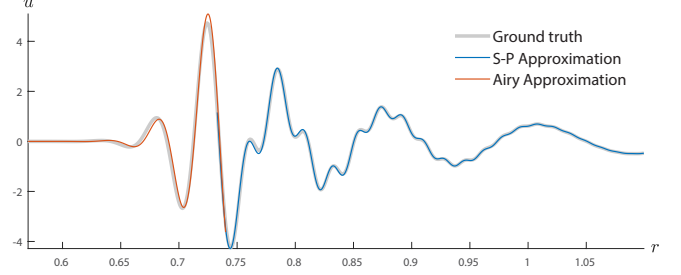


Fig. 2. Two-wave approximation and trailing-wave Airy approximation overlaid on ground truth. Graph shows rescaled surface height  $u$  as a function of distance to the impact  $r$ , four seconds after impact.

approximation for  $J_0(kr)$ , can be rewritten as

$$\begin{aligned} \theta(r, t) &\approx \int_0^\infty A(k) \cos\left(\omega(k)t - kr - \frac{\pi}{4}\right) dk, \\ A(k) &= \frac{\omega(k)J_2(k)D(k)}{\sqrt{2\pi k^3 r}}, \end{aligned} \quad (2)$$

where  $A(k)$  contains all factors that do not oscillate strongly.

The stationary-phase approximation predicts that the integrand only contributes to the value of  $\theta$  around  $k_1$  and  $k_2$ , and that the amplitude can be assumed constant for either contribution. We expand the phase around  $k_n$  with  $n = 1, 2$  in a second-order Taylor approximation, which gives

$$\begin{aligned} \phi(k) &\approx \phi(k_n) + \frac{1}{2}\phi''(k_n)(k - k_n)^2 \\ &= \omega(k_n)t - k_n r - \frac{\pi}{4} + \frac{1}{2}c'_g(k_n)t(k - k_n)^2. \end{aligned} \quad (3)$$

The contribution of either wavenumber is computed separately and summed in the end. Since  $k_1, k_2 > 0$ , the lower integration limit can be extended to  $-\infty$  without violating the assumptions of the stationary-phase approximation. This gives, after shifting the integration variable by  $k_n$ ,

$$\theta(r, t) \approx \sum_{n=1}^2 A(k_n) \int_{-\infty}^\infty \cos\left(\omega(k_n)t - k_n r - \frac{\pi}{4} + \frac{1}{2}c'_g(k_n)t k^2\right) dk. \quad (4)$$

This last integral can be expressed in closed form as a short computation shows.

$$\begin{aligned} &\int_{-\infty}^\infty \cos\left(\omega(k_n)t - k_n r - \frac{\pi}{4} + \frac{1}{2}c'_g(k_n)t k^2\right) dk \\ &= \Re \left\{ \exp\left(i\left(\omega(k_n)t - k_n r - \frac{\pi}{4}\right)\right) \int_{-\infty}^\infty \exp\left(i\frac{1}{2}c'_g(k_n)t k^2\right) dk \right\}. \end{aligned} \quad (5)$$

The integral in this last expression is a Fresnel integral. Using the shorthand  $B_n = \frac{1}{2}c'_g(k_n)t$ , it evaluates to

$$\int_{-\infty}^\infty \exp\left(iB_n k^2\right) dk = \sqrt{\frac{\pi}{2|B_n|}} (1 + i \operatorname{sgn}(B_n)).$$

Only the sign of the imaginary part depends on the sign of  $B_n$  because sine is an odd function while cosine is even.

Next, we make use of the relations

$$\Re \left\{ \exp \left( i \left( x - \frac{\pi}{4} \right) \right) (1 + s i) \right\} = \begin{cases} \sqrt{2} \cos(x) & \text{if } s = 1, \\ \sqrt{2} \sin(x) & \text{if } s = -1 \end{cases}$$

and solve the Fresnel integral to rewrite Eq. 5 as

$$\sqrt{\frac{\pi}{|B_n|}} \text{trig}_n(\omega(k_n)t - k_n r),$$

where  $\text{trig}_1 = \sin$  and  $\text{trig}_2 = \cos$ . This is because the sign of  $B_n$  is the same as the sign of  $c'_g$ , which, as seen in Fig. 1, is negative for  $k_1$  and positive for  $k_2$ .

With this result, and by using the expansion  $J_2 \approx \frac{1}{8}k^2$ , we can finally rewrite Eq. 4 as

$$\theta(r, t) \approx \sum_{n=1}^2 \frac{\omega(k_n)D(k_n)\sqrt{k_n}}{8\sqrt{rt|c'_g(k_n)|}} \text{trig}_n(\omega(k_n)t - k_n r). \quad (6)$$

Evaluating one of the two terms in this sum is approximately as expensive as evaluating the integrand in Eq. 2. But since the integrand is oscillatory, approximating the integral in Eq. 2 via numerical quadrature would take many more than two samples to achieve a similar level of accuracy.

The only extra effort that the stationary-phase approximation requires is the computation of  $k_1$  and  $k_2$  as the solutions to  $c_g(k) = \frac{r}{t}$ . Since  $c_g$  is well-behaved, we can precompute a lookup table for the roots of  $c_g(k) - \frac{r}{t}$  as a function of  $\frac{r}{t}$  to, e.g., query dominant wavenumbers from the GPU.

### 3.2 Trailing-wave approximation

If  $\frac{r}{t}$  is very close to the minimal group speed  $c_{g,\min}$ , the two-wave approximation is no longer accurate, because the contribution ranges of  $k_1$  and  $k_2$  overlap, and cannot be treated independently. Mathematically, as  $\frac{r}{t}$  tends to  $c_{g,\min}$ , the group speed derivatives  $c'_g(k_1)$  and  $c'_g(k_2)$  tend to zero, and the approximation in Eq. 6 tends to  $+\infty$  or  $-\infty$ .

A way to treat the case  $\frac{r}{t} < c_{g,\min} + \varepsilon$  is to use a third-order Taylor expansion of the phase function at  $k_0$ , where  $c_{g,\min} = c_g(k_0)$ , which reads

$$\begin{aligned} \phi(k) &\approx \phi(k_0) + \phi'(k_0)(k - k_0) + \frac{1}{6}\phi^{(3)}(k_0)(k - k_0)^3 \\ &= \alpha + \beta(k - k_0) + \gamma(k - k_0)^3, \end{aligned}$$

$$\text{with } \alpha = \omega(k_0)t - k_0 r - \frac{\pi}{4}, \quad \beta = c_{g,\min}t - r, \quad \gamma = \frac{1}{6}c''_g(k_0)t.$$

As with the two-wave approximation, we replace the phase function in Eq. 2 by its expansion and extend the lower integration bound to  $-\infty$ . This gives

$$\theta(r, t) \approx A(k_0) \Re \left\{ \exp(i\alpha) \int_{-\infty}^{\infty} \exp \left( i \left( \beta k + \gamma k^3 \right) \right) dk \right\}. \quad (7)$$

The integral in this expression can be written in analytic form using the Airy function

$$\text{Ai}(x) = \frac{1}{\pi} \int_0^{\infty} \cos \left( \frac{t^3}{3} + xt \right) dt.$$

This is achieved by substituting  $l = (3\gamma)^{1/3}k$  in Eq. 7.

$$\begin{aligned} &\int_{-\infty}^{\infty} \exp \left( i \left( \beta k + \gamma k^3 \right) \right) dk \\ &= (3\gamma)^{-1/3} \int_{-\infty}^{\infty} \exp \left( i \left( \frac{l^3}{3} + \beta(3\gamma)^{-1/3}l \right) \right) dl \\ &= 2\pi(3\gamma)^{-1/3} \text{Ai} \left( \beta(3\gamma)^{-1/3} \right). \end{aligned}$$

Note that this expression is real, because the imaginary part of the integrand is an odd function.

Substituting the result into Eq. 7 gives the final expression

$$\theta(r, t) \approx 2\pi(3\gamma)^{-1/3} A(k_0) \cos(\alpha) \text{Ai} \left( \beta(3\gamma)^{-1/3} \right). \quad (8)$$

As noted above, the characteristic appearance of gravity-capillary rings is captured by the two-wave approximation. Therefore, the accompanying video simply fades the two-wave approximation to zero at the trailing edge. To still use Eq. 8 in a real-time application, the Airy function needs to be evaluated for arguments around zero. This can be done either with a precomputed lookup table or with an asymptotic expansion at zero.

## 4 IMPLEMENTATION

This second-order approximation was implemented in a real-time graphics application to demonstrate that this formulation can be used to simulate hundreds of wave rings at 60 frames per second. Computation and rendering is performed in three passes.

- (1) For every wave on screen, the radius  $r$  is sampled uniformly in the range corresponding to the minimum group speed and a cut-off value, at which damping is so strong that the waves are visually imperceptible. For each wave and each sample, the wave height is evaluated in parallel using a computer shader program. The results are stored in a 2d texture, with every row containing the samples of one wave.
- (2) This pass transfers the wave height information onto a one-channel screen-space texture that contains the cumulative wave height for every pixel. Every wave is rendered as a bounding quad into this texture, with the wave height at each pixel as the output color. The blending capability of the GPU is used to additively accumulate waves whose bounding quads overlap in screen-space.
- (3) Finally, the waves are rendered onto the screen following the projected-grid idea of Johanson and Lejdfors [2004].

A more detailed description of the implementation is available in the form of code comments. The relevant files are

- `RippleApp.cpp`: initialization, user interface, update/draw loop, Pass 3
- `WaveComputations.cpp`: Pass 1
- `WaveQuadRenderer.cpp`: Pass 2

The shader code can be found in `compute_wave.comp` (Pass 1), `waves.vs`, `waves.fs` (Pass 2), `basic.vs`, `basic.fs` (Pass 3). The readme provides a guide to set up the demo in Visual Studio 2017, and an overview of the controls.

The second-order and third-order approximations are also implemented in Matlab as an interactive demo. To start the demo, execute `init_paths; Wave()`; in the directory containing the Matlab files.

## REFERENCES

- Claes Johanson and Calle Lejdfors. 2004. *Real-time water rendering*. Master's thesis. Lund University.
- Bernard Le Méhauté. 1988. Gravity-capillary rings generated by water drops. *Journal of Fluid Mechanics* 197 (1988), 415–427.

## A COMPUTATION SUMMARY

This section summarizes all formulae involved in the computation of raindrop ripples. It serves as a reference for implementation and allows to skip the derivations above.

First, we establish all physical constants, and variables in their dimensionless and dimensionalized form. Dimensionalized quantities will be denoted with a \*-superscript, and dimensionless quantities without.

The radius of a raindrop is denoted by  $R^*$ , and is typically around  $2 \cdot 10^{-3}$  m. Other constants are the gravitational acceleration  $g^* = 9.8 \text{ m/s}^2$ , the density of water  $\rho^* = 10^3 \text{ kg/m}^3$ , the surface tension of water  $\tau^* = 7.4 \cdot 10^{-2} \text{ N/m}$ , the kinematic viscosity of water  $\nu^* = 10^{-6} \text{ m}^2/\text{s}$ , and the terminal velocity of a raindrop  $W^* = 10 \text{ m/s}$ .

Important variable quantities are the distance to the impact location  $r$ , the time since the impact  $t$ , the surface height  $u(r, t)$ , the wavenumber  $k$ , and the angular frequency  $\omega(k)$ . Most equations are written in terms of dimensionless variables, but we list all conversions here.

$$r = \frac{r^*}{R^*}, \quad t = t^* \sqrt{\frac{g^*}{R^*}}, \quad u = \frac{u^*}{R^*}, \quad k = R^* k^*,$$

$$\omega = \omega^* \sqrt{\frac{R^*}{g^*}}, \quad \tau = \frac{\tau^*}{\rho^* g^* R^{*2}}, \quad W = \frac{W^*}{\sqrt{g^* R^*}}.$$

The angular frequency  $\omega$  of a wave depends only on its wavenumber  $k$ . The group speed  $c_g$  of a wave is the derivative of  $\omega$  with respect to  $k$ . The first derivative of  $c_g$  is required for the two-wave approximation, and the second derivative needs to be evaluated at a single location for the trailing-wave approximation. These quantities are given by

$$\omega = \sqrt{k(1 + \tau k^2)}, \quad c_g = \frac{d\omega}{dk} = \frac{3k^2\tau + 1}{2\sqrt{k^3t + k}},$$

$$c'_g = \frac{3k^2t(k^2t + 2) - 1}{4(k^3t + k)^{3/2}}, \quad c''_g = -\frac{3(k^2t - 1)(k^2t + 6) + 1}{8(k^3t + k)^{5/2}}.$$

We identify some important quantities that are derived from these functions. The minimum group speed  $c_{g,\min}$  is defined as the unique minimum of  $c_g$ , attained at the wavenumber  $k_0$ , i.e.,  $c'_g(k_0) = 0$  and  $c_g(k_0) = c_{g,\min}$ . Both  $k_0$  and  $c_{g,\min}$  can be precomputed. We also define  $k_1$  and  $k_2$  as the two unique roots of the function  $c_g - \frac{r}{t}$ , with  $k_1 < k_2$ . These roots exist for  $\frac{r}{t} > c_{g,\min}$  and can be precomputed for all relevant values of  $\frac{r}{t}$  and stored in a look-up table. It suffices to precompute  $k_1$  and  $k_2$  for  $\frac{r}{t} \in [c_{g,\min}, 3c_{g,\min}]$  because waves outside this range will be too heavily damped to be visible.

The damping function  $D$  and the damping coefficient  $\gamma^*$  are expressed in terms of the dimensionalized wavenumber  $k^*$  and its angular frequency  $\omega^*$ :

$$D(k^*) = \exp(-\gamma^* t^*), \quad \text{with} \quad \gamma^* = \frac{1}{2} \sqrt{\frac{\omega^* \nu^*}{2}} k^* + 2\nu^* k^{*2}.$$

The two-wave approximation for the waveheight reads

$$u(r, t) \approx \frac{3W}{128\sqrt{rt}} [A(k_1) \sin(\omega(k_1)t - k_1 r) + A(k_2) \cos(\omega(k_2)t - k_2 r)],$$

$$\text{with } A(k) = \frac{\omega(k)D(k^*)\sqrt{k}}{\sqrt{|c'_g(k)|}}.$$

The trailing-wave approximation for the waveheight reads

$$u(r, t) \approx \frac{C a(t)}{\sqrt{r}} \cos\left(\omega(k_0)t - k_0 r - \frac{\pi}{4}\right) \text{Ai}[(c_{g,\min} t - r) a(t)],$$

$$\text{with } C = \frac{3W\omega(k_0)D(k_0^*)\sqrt{\pi k_0}}{64\sqrt{2}}, \quad a(t) = \left(\frac{1}{2}c''_g(k_0)t\right)^{-1/3},$$

where  $C$  and  $c''_g(k_0)$  can be precomputed.